
FadMan: Federated Anomaly Detection across Multiple Attributed Networks

Nannan Wu
Tianjin University
China
nannan.wu@tju.edu.cn

Ning Zhang
Tianjin University
China
2020244106@tju.edu.cn

Wenjun Wang
Tianjin University
China
wjwang@tju.edu.cn

Lixin Fan
WeBank
China
lixinfan@webank.com

Qiang Yang
WeBanky
China
qyang@cse.ust.hk

Abstract

Anomaly subgraph detection has been widely used in various applications, ranging from cyber attack in computer networks to malicious activities in social networks. Despite an increasing need for federated anomaly detection across multiple attributed networks, only a limited number of approaches are available for this problem. Federated anomaly detection faces two major challenges. One is that isolated data in most industries are restricted share with others for data privacy and security. The other is most of the centralized approaches training based on data integration. The main idea of federated anomaly detection is aligning private anomalies from local data owners on the public anomalies from the attributed network in the server through public anomalies to federate local anomalies. In each private attributed network, the detected anomaly subgraph is aligned with an anomaly subgraph in the public attributed network. The significant public anomaly subgraphs are selected for federated private anomalies while preventing local private data leakage. The proposed algorithm FADMAN is a vertical federated learning framework for public node aligned with many private nodes of different features, and is validated on two tasks — correlated anomaly detection on multiple attributed networks and anomaly detection on an attributeless network — using five real-world datasets. In the first scenario, FADMAN outperforms competitive methods by at least 12% accuracy at 10% noise level. In the second scenario, by analyzing the distribution of abnormal nodes, we find that the nodes of traffic anomalies are associated with the event of *postgraduate entrance examination* on the same day.

1 Introduction

The anomaly detection problem has recently attracted much more attention. Many machine learning methods have been proposed to spot anomalies in different scenarios, such as disease outbreak detection in health alert networks, traffic jam detection in road networks, and event detection in social networks [Kulldorff, 1997, Speakman et al., 2015, 2013, Takahashi et al., 2008, Wu et al., 2018, Chen et al., 2019a, Parkinson et al., 2018]. Most of the current methods are just used to centralized data. However, most industry data exist in the form of isolated islands [Yang et al., 2019]. Few solutions are proposed to the federated anomaly detection problems that are applied among multiple attributed networks without compromising user privacy¹. Recently, anomaly detection methods are proposed to multiple networks without considering data privacy [Bindu et al., 2017, Szmit et al., 2012]. These methods are focused on anomalies with the same anomaly characteristics on multiple attributed

¹In this paper, we use ‘graph’ and ‘network’, ‘vertex’ and ‘node’, and ‘attribute’ and ‘feature’ interchangeably. Preprint. Under review.

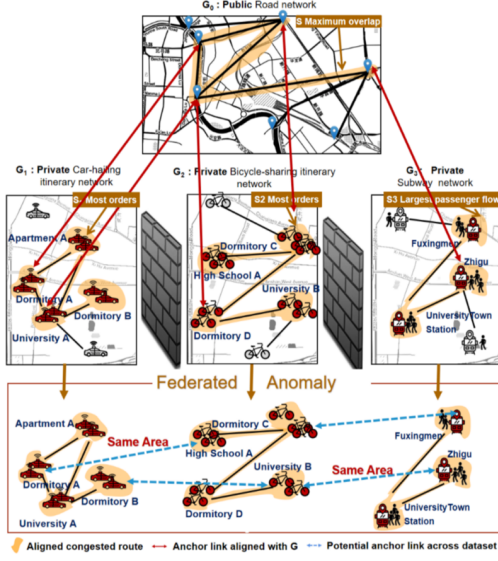


Figure 1: **Federated anomaly passenger flow** itineraries with similar structures in three private industry traffic datasets (Car-hailing & Bicycle-sharing & Subway). The federated anomaly is highly correlated (blue lines) in geographic attributes and specific locations (yellow shades).

networks in a specific field, and the accuracy improvement of the overall anomaly detection [Sun et al., 2020, Futamura et al., 2020]. The work [Bindu et al., 2017] focuses on multi-layer social networks and uses hierarchical information to assist the overall abnormal ranking of nodes, which lacks analyses of the correlation abnormalities among different social networks.

Attributed graph becomes more popular in industry data, which exhibit graph structure and node feature heterogeneity. We find that different graph anomalies, even from the same industry or same dataset, are non-IID on both structures and node features. Most industries protect the heterogeneity for the private reasons, e.g., a car-hailing company protects its travel demand network heterogeneity. It is a challenge to find the anomaly associations on multiple private attributed networks, and few further explorations have been carried out on multiple private attributed networks for the federated anomaly detection [Zhao et al., 2019, Chen et al., 2019b, Ying et al., 2021, Zhao et al., 2020]. In Figure 1, our proposed FADMAN pays attention to federated anomalies of multiple private attributed networks and their potential correlations in various fields without compromising data privacy. We can observe that the “the largest passenger flow” subway station network aligning with “the most car-hailing and bicycle-sharing orders”, which means that most people arrive or leave at a subway station with transfer to bicycle or car at the certain relevant location. In n industries, there are multiple private attributed networks, $\{G_1, \dots, G_N\}$. A well-known cost function $F_\alpha(S)$ for $S \subseteq G_i$ can be specifically modeled in the i th industry data to detect the anomaly. We select a public attributed network G_0 , and present an alignment function $Q_\sigma(S, U)$ for $U \subseteq G_0$ to align the private anomaly S on the public anomaly U . F is the abnormal score of S (e.g., the work Tree-Shape-Priors Subgraph Detection (TSPSD) [Wu et al., 2018] as F). Q is the alignment score of S and U (e.g., the work Cross-Network Embedding for Multi-Network Alignment (CrossMNA) [Chu et al., 2019] as Q). The parameters α and σ are significant level and alignment threshold respectively.

Related work. Anomaly detection has been extensively studied from outlier detection, anomaly subgraph detection in one attributed network and multiple attributed networks to federated anomaly detection in multiple isolated attributed networks. Most of these algorithms are used in a single attributed network [Cadena et al., 2018, Bhatia et al., 2020, Cai et al., 2020, Boniol and Palpanas, 2020]. A few algorithms are used in multi-layer networks [Bindu et al., 2017, De Domenico et al., 2015, Tam et al., 2019, Jie et al., 2020] for abnormal nodes. The methods based on network alignment are used to multi-layer networks for anomaly subgraph detection [Sun et al., 2020, Zhang et al., 2015, Liu et al., 2014, Heimann et al., 2018, Ye et al., 2019, Huynh et al., 2019, Yan et al., 2021, Sun et al., 2019, Wang et al., 2018b, Meng et al., 2019]. Many federated learning methods on graphs are proposed to explore graph embedding vectors average [Xie et al., 2021, Li et al., 2020b, 2021, Zhang et al., 2021]. However, the transmitted gradient parameters are still at risk of data leakage [Zhu et al., 2019, Lyu et al., 2020, Melis et al., 2019]. There are approaches that tackle statistical heterogeneity

Algorithm 1: FADMAN

Input : $\mathbb{G} = \{G_0, G_1, \dots, G_N\}, \alpha, \sigma$

Output : aligned anomaly subgraph U

```

1 Initiate variables  $i = 0, U^i = \emptyset$ ;
2 while  $U^i \neq U^{i+1}$  do
3   /* Participant side */;
4   for  $j = 1, 2, \dots, N$  do
5      $S_j^* \leftarrow \arg \max F_\alpha(S) + Q_\sigma(S, U^i)$ , for  $S \subseteq G_j$ ;
6      $U_j^* \leftarrow \arg \max Q_\sigma(S_j^*, U)$ , for  $U \subseteq G_0$ ;
7   end
8   /* Server side */;
9    $U^{i+1} \leftarrow \arg \max \sum_{j=1}^N Q_\sigma(S_j^*, U)$ , for  $U \subseteq U^*$ ;
10   $i \leftarrow i + 1$ ;
11 end
```

by considering local partial data or some server-side proxy data as model parameters [Li et al., 2020a, Xie et al., 2021]. We are motivated on private anomalies aligning on public anomaly to protect data privacy and federate local anomalies. We summarize our main contributions as follows:

- **Innovative work.** A novel pioneer algorithm is first proposed to federated anomaly detection on multiple attributed networks in the vertical federated learning without compromising data privacy.
- **Theoretical guarantee.** The proposed algorithm enjoys a proved convergence property. A broad spectrum of anomaly detection functions is applicable under satisfying the function properties. Specifically, for the graph scan statistics (e.g., Berk-Jones), the algorithm succeeds in federated anomaly detection with car-hailing, bicycle-sharing and subway industry data.
- **Effectiveness and robustness.** Extensive experiments on real datasets have verified that FADMAN can be effectively applied to different multi-network scenarios. On the real computer network dataset, our method achieves 97% accuracy at the ten percent noise level, which is 12% higher than the competitive methods in accuracy.

2 Problem formulation

A data owner has an attributed network $G = (V, E, P)$, $V = \{v_1, \dots, v_n\}$, $E \subseteq V \times V$ are sets of vertices and edges in G , and $P \in \mathbb{R}^n$ is the specific anomaly feature set of G . P is widely obtained by the mapping function $\mathbf{p} : V \rightarrow [0, 1]$ defines the empirical p-value corresponding to each node $v \in V$ [Wu et al., 2018, Chen and Neill, 2014], the smaller the p-value, the more abnormal the node. Anomaly target detection can be represented as identifying subgraphs $S \subseteq G$ whose vertex set V_S and edge set E_S are subset of V, E .

We consider a set of data owners denoted by $\{G_1, G_2, \dots, G_N\}$ as multiple attributed networks. One global anomaly $\{S_1, S_2, \dots, S_N\}$ (e.g., anomaly transportation in a city) is distributed as local anomalies on multiple attributed networks. We denote $[N]$ as the set of $\{1, 2, \dots, N\}$. The local anomaly S_i for $i \in [N]$ can be identified by maximizing the local model $F_\alpha^i(S_i)$ with the significant level α . We introduce a public data owner G_0 to bridge the gap among isolated private data owners. A public anomaly $U \subseteq G_0$ instead of the global anomaly is associated with local anomalies. An local alignment function $Q_\sigma^i(S_i, U)$ is employed to measure the similarity between S_i and U for $i \in [N]$. For anomaly subgraphs $S_i \subseteq G_i$ and $U \subseteq G_0$, each private data owner exclusively defines the alignment matrix $A^i \in \{0, 1\}^{n \times n}$, where $A_{uw}^i \leftarrow 1$ if the value of (u, w) is greater than the alignment threshold σ (i.e., a constant) with $u \in V_{S_i}$ and $w \in V_U$, $A_{uw}^i \leftarrow 0$ otherwise.

Federated anomaly detection problem. The federated anomaly detection across multiple attributed networks can be formulated as follows:

$$(S^*, U^*) = \arg \max_{U \subseteq G_0} \sum_{i=1}^N \max_{S_i \subseteq G_i} F_\alpha^i(S_i) + Q_\sigma^i(S_i, U) \quad (1)$$

where the private anomaly subgraphs S^* and the public anomaly subgraph U^* are the optimal solutions. The private anomaly subgraph $S_i \subseteq G_i$ is measured by F with the significant level α (e.g., 0.15). The alignment score between S_i and the public anomaly U is measured by Q with the predefined alignment threshold σ (e.g., 0.8). For the optimization problem (1), we can assume that the desired anomalies $\{S_i\}$, U , and the functions F_α^i, Q_σ^i , intuitively satisfy the four properties:

- (P1) F_α^i is monotonically **increased** with the number of abnormal nodes in S_i ;
- (P2) F_α^i is monotonically **decreased** with the number of normal nodes in S_i ;
- (P3) Q_σ^i is monotonically **increased** with the number of node pairs aligned between S_i and U ;
- (P4) Q_σ^i is monotonically **decreased** with the number of nodes from S_i and U .

These properties P1-P2 are widely used in connected anomaly subgraph detection [Chen and Neill, 2014, Wu et al., 2018], and the possibility of same anomaly is increased with aligned links P3 [Sun et al., 2020]. We can observe that when the anomaly U is the whole graph G_0 , there are maximum links between S_i and U by the property P3. The anomaly U is not desired for including more noise (i.e., normal nodes). Similarly, we have S_i . In this work, we include the property P4, which restricts on the smaller sizes of anomalies S_i and U .

3 Proposed algorithm

The federated anomaly detection problem (1) does not explicitly allow for data protection in different data owners. We propose the algorithm that is tractable to protect data and detect federated anomaly. The key idea of proposed algorithm is to aggregate local public anomalies and then re-distribute the optimized public anomaly back to each local data owner.

3.1 Federated anomaly detection

The main steps of the FADMAN in Algorithm 1 are described as follows:

For the i -th participant side (local data owner), given the optimized public anomaly U ,

$$(c1) S_i^* \leftarrow \arg \max_{S \subseteq G_i} F_\alpha^i(S) + Q_\sigma^i(S, U)$$

$$(c2) U_i^* \leftarrow \arg \max_{U \subseteq G_0} Q_\sigma^i(S_i^*, U)$$

For the server side, aggregate local public optimized anomalies $\{U_i^*\}$ for $i \in [N]$,

(s1) Sort the local data owner $U_{(i)}^*$ in ascending order of size $|V_{U_{(i)}^*}|$

(s2) For a coalition $C = \{\}$, start at the owner i joining the coalition C , and stop when the first owner would increase the alignment error $(\sum_{k \in C} |V_{U_k^*}| - |V_{U_{(i)}^*}|) / (|V_{U_{(i)}^*}| \sum_{k \in C} |V_{U_k^*}|) Q_\sigma^i(S_{(i)}^*, U_{(i)}^*)$ by joining the coalition C . Then, the optimal partition of $[N]$ is made up of the coalition set $\{C\}$.

(s3) Select a coalition C with the minimum score, and set the new public anomaly $U = \bigcup_{i \in C} U_{(i)}^*$

We can observe that the private data $\{S_i\}$ at the local data owners would not be uploaded to the server. At the server side, we can just obtain the public anomalies $\{U_i^*\}$ and its alignment scores. The problem is solved with two different settings: *participant side* for private anomaly detection has N data owners who do not share data with each other; and *server side* for public anomaly alignment has the public attributed network which is shared by the data owners. Algorithm 1 is iterated between the participant side and the server side, until the stop condition is satisfied (i.e., the public anomaly subgraph U does not change).

3.1.1 Private anomaly detection.

Each data owner employs a function F to detect self-defined anomaly by consolidating their private attributed network data. The self-defined anomaly at step 5 and step 6 of Algorithm 1 is detected exclusively in the data owner setting. The anomaly detection provides meaningful privacy guarantees. In this paper, we employ the non-parametric graph scanning statistic F as a score function, and its form is defined as follows:

$$F_\alpha(S) = \varphi(\alpha, N_\alpha(S), N(S)). \quad (2)$$

where S is a set of connected vertices, that is, a subgraph, and α is the significant level, $N_\alpha(S)$ is the number of anomaly vertices in S whose p-value is less than or equal to α , and $N(S)$ is the total number of vertices in S . In this paper, we consider two non-parametric graph scanning statistics as the score function (2): Berk-Jones (BJ) statistic [Berk and Jones, 1979] and Higher Criticism (HC) statistic [Donoho et al., 2004]. We use non-parametric graph scanning statistics to measure the subgraph abnormality as a numerical value. The optimal anomaly subgraphs maximize the graph scanning statistics F over each private network.

3.1.2 Public anomaly alignment.

Given the public attributed network G_0 and another attributed network G_i for $i \in \{0, 1, \dots, N\}$, we define the function Q as measuring the anomaly alignment score between $S \subseteq G_i$ and $U \subseteq G_0$:

$$Q_\sigma(S, U) = \frac{N_\sigma(S, U)}{N(S)} + \frac{N_\sigma(S, U)}{N(U)} \quad (3)$$

where σ is the predefined alignment threshold. The anomaly subgraph S is aligned on the public anomaly subgraph U . The two subgraphs are connected. $N_\sigma(S, U)$ is the number of node pairs between S and U whose alignment probability is greater than or equal to σ . $N(S)$ and $N(U)$ are the number of all nodes in S and U respectively. The node's alignment probability is obtained through the

network alignment work CrossMNA [Chu et al., 2019]. By introducing this algorithm, we pre-aligned each private network with the public network, and obtained the alignment probability of all pairs of nodes between them. We use network alignment to map the similarity between the subgraphs to a value, and obtain the most similar part between two subgraphs by maximizing Q at step 6, 9 of Algorithm 1.

3.2 Theoretical analysis

We now analyze the increasing property in the objective when one iteration of the proposed algorithm is performed. The convergence of FADMAN is proved based on several lemmas and the four properties of objective function, without the specific forms of F and Q functions. Each lemma is a building-block that describes that there exists an local optimal solution.

Theorem 1 (Convergence and Optimality of FADMAN). *Within the pre-aligned domain (each data owner integrates the alignment probability information of all node pairs between its private network and the public network), given the parameter α and σ settings, Algorithm 1 converges to the optimal solution of the problem (1).*

Though Theorem 1 looks straightforward to a network-based algorithm framework for federated anomaly detection, the problems at steps (c1) and (c2) can be addressed with the previous methods Sun et al. [2020], Wu et al. [2018] support the optimal solutions. At the step (c1), given the public anomaly U , the optimal private anomaly S_i^* is obtained. We are target for the new improved public anomaly U at the next iteration.

At the t -th iteration, for the server side, we can observe the public anomalies $\{U_i^*\}$ and the function values of F and Q . We assume that there exists a public anomaly subgraph $U^* \subseteq G_0$ maximizing $\sum_{i \in [N]} Q_\sigma^i(S_i^*, U^*)$ under the fixed S_i^* . The value of $F_\alpha^i(S_i^*)$ will not change with the update U .

Lemma 2 (Q upper bound). *We must have the upper bound of the optimal Q under the fixed S_i^* .*

$$\sum_{i=1}^N Q_\sigma^i(S_i^*, U_i^*) \geq \sum_{i=1}^N Q_\sigma^i(S_i^*, U^*). \quad (4)$$

Lemma 3 (Q lower bound). *A public anomaly $U^o \subseteq \bigcup_{i \in [N]} U_i^*$ maximizes $\sum_{i \in [N]} Q_\sigma^i(S_i^*, U^o)$. We must have the lower bound of the optimal Q under the fixed S_i^* .*

$$\sum_{i=1}^N Q_\sigma^i(S_i^*, U^o) \geq \sum_{i=1}^N Q_\sigma^i(S_i^*, U^*). \quad (5)$$

Lemma 4 (Q optimum solution). *The solution $U^o = U^*$ maximizes Q under the fixed S_i^* over G_0 . The optimum solution must exist between*

$$\min_{U \subseteq \bigcup_{i \in [N]} U_i^*} \sum_{i=1}^N \left[Q_\sigma^i(S_i^*, U_i^*) - Q_\sigma^i(S_i^*, U) \right] \quad (6)$$

The public anomaly U_i^* is the local maximum solution. The Q upper bound is derived intuitively from summing local maximum solutions is greater than the global maximum solution. For the Q lower bound, the maximum solution over the local set is less than or equal the maximum solution over the global set. We can observe that the maximum solution must exist between the upper bound and lower bound, and minimize the gap between the two bounds. Note that when the gap is 0, the optimum solution is equal to the solution of lower bound. All of the local solutions U_i^* are the same.

However, in the problem (6), $Q_\sigma^i(S_i^*, U)$ can not be computed at the server because the forms of function Q and private anomalies $\{S_i^*\}$ are not accessed for the data protection rules. We employ the framework for optimality and stability in federated learning to address the problem (6) Donahue and Kleinberg [2021]. We define a coalition $C \subseteq [N]$ is a subset of local data owners, and all owners $[N]$ are partitioned into coalition set $\{C\}$. We consider the gap between two bounds (6) as errors across

Dataset	Division rule	Time (YYYYMMDD)	Graph	Vertex		Edge	
				property	#	property	#
Computer Network	time	20140531-20140731	G1	IP/website	2,639	IP visited the website	4,203
		20140801-20140930	G2		1,963		2,887
		20141001-20141131	G3		2,012		3,528
		20141201-20150131	G4		2,192		3,860
		20150201-20150331	G5		1,330		2,069
		20150401-20150531	G6		124,089		165,224
<i>Car-Hailing</i>	traffic type	20191221 0:00-24:00	G1	itinerary start/end point	54,962	the same itinerary	158,674
<i>Bicycle-Sharing</i>		20191221 0:00-24:00	G2		20,858		229,816
<i>SubWay (Metro)</i>		20191221 0:00-24:00	G3	station	143		subway line

Table1: Summary of Datasets.

owners. By the properties P3 and P4, we know that the value of $Q_\sigma^i(S_i^*, U)$ changed with the size of U for the fixed S_i^* . Given a partition Π of $[N]$, we define its error below:

$$f_{\{U_i^*\}}(\Pi) = \sum_{C \in \Pi} \sum_{i \in C} |V_{U_i^*}| \cdot \left(\frac{\sum_{k \in C} |V_{U_k^*}| - |V_{U_i^*}|}{|V_{U_i^*}| \cdot \sum_{k \in C} |V_{U_k^*}|} \right) Q_\sigma^i(S_i^*, U_i^*) \quad (7)$$

Lemma 5 (Theorem 1, from Donahue and Kleinberg [2021]). *An optimal partition Π can be created for a set of local data owners $[N]$. First, start with every owner maximizing the local public anomaly U_i^* . Then, group the owners together in ascending order of node size, halting at the first owner would increase its error $(\sum_{k \in C} |V_{U_k^*}| - |V_{U_i^*}|) / (|V_{U_i^*}| \sum_{k \in C} |V_{U_k^*}|) Q_\sigma^i(S_i^*, U_i^*)$ by joining the coalition C . The resulting partition Π is optimal.*

By Lemma 5, we select a coalition $C \in \Pi$ with the minimum error, and achieve the desired public anomaly $U = \bigcup_{i \in C} U_i^*$. The public anomaly U is the optimal solution for $\sum_{i \in [N]} Q_\sigma^i(S_i^*, \cdot)$.

Note that the bi-level optimization problem (1) has two targets. The local function $F_\alpha^i(S_i)$ aims to detect private anomalies using only the data of local data owner i . The alignment function $Q_\sigma^i(S_i^*, U_i^*)$ aims to federate these anomalies by aligning the local private anomaly on the public global anomaly. We can observe that the two functions exhibit at two scales, and introduce a hyperparameter λ , $\max_{U \subseteq G_0} \sum_{i \in [N]} \max_{S_i \subseteq G_i} F_\alpha^i(S_i) + \lambda Q_\sigma^i(S_i, U)$, controls the interpolation between the two functions. The hyperparameter λ is related to the specific form of Q , e.g., Q as a regularization term, and the theoretical properties of FADMAN is proved under the general setting without λ . When λ is set to 0, our algorithm performs as local anomaly detection tasks for each local data owner. Our algorithm focuses on more federated anomalies with increasing λ .

(Relation to Ditto federated learning Li et al. [2021]). We do not consider the network structure $\{G_i\}$, and each G_i can be transformed to a vector v_i , e.g., $v_i(k) \leftarrow 1$ if the node k is abnormal in G_i , and $v_i(k) \leftarrow 0$ otherwise. The vector w is derived from G_0 . We can take Q as a regularization term, $\lambda/2 \cdot \|Av_i - w\|^2$. The optimization problem is to minimize $-F_i(v_i) + \lambda/2 \cdot \|Av_i - w^*\|^2$ for v_i with each owner, subject to $w^* = \arg \min_w 1/N \cdot \sum_{i \in [N]} \|Av_i - w\|^2$. Our algorithm can be reduced to Ditto. Thus we propose a general algorithm framework for federated anomaly detection.

By the theorem, our algorithm guarantees on detecting the most anomaly subgraphs on multiple private attributed networks. FADMAN's time complexity is $O(kN|V|^2)$, where k is the number of iterations, N is the number of networks, V is the number of nodes of the network. In practice, the implementations of F_α and Q_σ are normalized because the function value ranges are different.

4 EXPERIMENTS

In this section, we performed a series of experiments to verify FADMAN. We applied the algorithm to two real scenarios and verified the effectiveness of the algorithm on the two tasks of correlated anomaly detection on multiple attributed networks and anomaly detection on an attributeless network through ground truth. We compared it with four competitive baselines.

Algorithms	Noise Ratio(%)	Precision	F1	Recall	TPR	FNR	Accuracy
FADMAN(BJ)-6	0	0.97	0.88	0.80	0.80	0.20	0.99
FADMAN(BJ)-6	10	0.97	0.87	0.79	0.79	0.21	0.97
FADMAN(BJ)-6	30	0.93	0.85	0.73	0.73	0.27	0.96
FADMAN(BJ)-3	0	0.97	0.85	0.76	0.76	0.24	0.99
FADMAN(BJ)-3	10	0.96	0.83	0.75	0.75	0.25	0.97
FADMAN(BJ)-3	30	0.92	0.82	0.7	0.7	0.30	0.95
A3MAN(BJ)[2021]	0	0.99	1.00	1.00	1.00	0	0.99
A3MAN(BJ)[2021]	10	0.99	0.98	0.97	0.97	0.03	0.97
A3MAN(BJ)[2021]	30	0.97	0.95	0.94	0.94	0.06	0.91
ASD-FT(BJ)[2020]	0	0.94	0.94	0.94	0.94	0.06	0.89
ASD-FT(BJ)[2020]	10	0.93	0.92	0.93	0.92	0.08	0.86
ASD-FT(BJ)[2020]	30	0.93	0.93	0.93	0.93	0.07	0.85
TSPSD(BJ)[2019]	0	0.95	0.97	0.96	0.96	0.04	0.95
TSPSD(BJ)[2019]	10	0.97	0.92	0.86	0.86	0.14	0.86
TSPSD(BJ)[2019]	30	0.95	0.81	0.70	0.70	0.30	0.69
NPHGS(BJ)[2014]	0	0.97	0.93	0.91	0.90	0.10	0.89
NPHGS(BJ)[2014]	10	0.95	0.88	0.82	0.82	0.18	0.80
NPHGS(BJ)[2014]	30	0.93	0.75	0.69	0.69	0.31	0.64

Table2: Comparison of Precision, F1, Recall, Accuracy, TPR (prediction) and FNR (prediction) on multiple attributed networks under the noise ratio = 0%, 10%, 30%. FADMAN (BJ)-6 denotes the experimental results for six networks from G1-G6, and FADMAN (BJ)-3 denotes the results for three networks from G4-G6.

Algorithms	Noise Ratio(%)	Anchor_Count	TPR(prediction)	FNR(prediction)
FADMAN(BJ)	0	1,012	0.98	0.02
FADMAN(BJ)	10	1,011	0.95	0.05
FADMAN(BJ)	30	1,010	0.93	0.07
ASD-FT(BJ)[2020]	0	115	0.94	0.06
ASD-FT(BJ)[2020]	10	74	0.88	0.08
ASD-FT(BJ)[2020]	30	16	0.86	0.07

Table3: Comparison of Anchor_Count, TPR (prediction) and FNR (prediction) on the attributeless network dataset under the noise ratio = 0%, 10%, 30%.

Datasets. We constructed two scenarios (Table 1) based on five real datasets: Computer network, Car-hailing & Bicycle-sharing & Subway (Metro) traffic & POI (Point of Interest) dataset. POI is the ground truth dataset to case study the federated anomaly association with interest locations.

In the first scenario, we divided the computer network into 6 private networks (with anomalous properties) according to time, treated the original network as a public network (only topology information), and conducted two comparative experiments on it: correlated anomaly detection on multiple attributed networks and anomaly detection on the attributeless network (regard G_6 as an attributeless network by setting the p-value of all nodes in G_6 to 1). In the second scenario, we use Car-hailing itinerary network, Bicycle-sharing itinerary network, and Subway network as the 3 private attributed networks, regard POI dataset as the public network. In this scenario, we conducted an experiment: correlated anomaly detection on multiple attributed networks.

Methods. In this work, we use anomaly detection algorithms NPHGS [Chen and Neill, 2014], TSPSD[Wu et al., 2018], A3MAN Zhang et al. [2018], and anomaly alignment algorithm ASD-FTSun et al. [2020] as baselines.

Metrics. We use Recall, Precision, F1, Accuracy, TPR (True Positive Rate), FNR (False Negative Rate) to evaluate algorithms' ability to detect the correlated anomaly on multiple attributed networks, and use Anchor_Count, TPR (prediction), FNR (prediction) to evaluate the algorithms' ability to detect anomalies on attributeless networks and discover related links among anomalies across the network (see supplementary in detail).

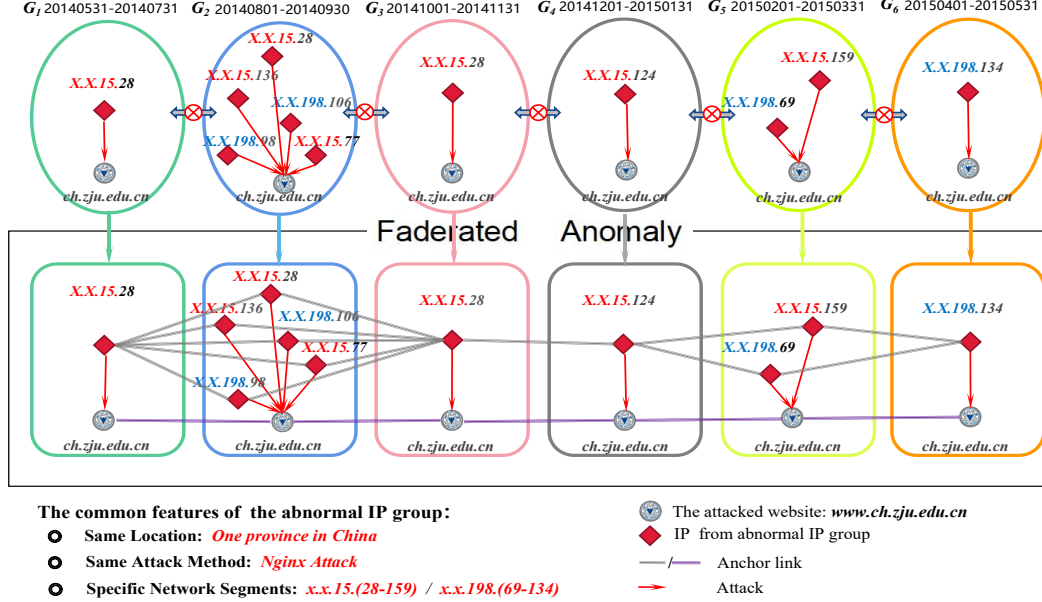


Figure 2: A set of related abnormal IPs was detected by our method. The detected IPs have potential correlations (e.g., at the same place). The site *www.ch.zju.edu.cn* was attacked mainly from two network segments *x.x.15.(28-159)* and *x.x.198.(69-134)*. The addresses of these IPs were all at the same place (i.e., *Shanxi, China*). The attack methods were all *Nginx Attack*.

4.1 Experiment results

We conduct comparative experiments on the computer network dataset with ground truth data, set $\alpha = 0.15$, $\sigma = 0.8$. The experimental results are shown in Table 2 and Table 3.

1) Ability to detect correlated anomalies on multiple attributed networks: Taking all the attributed computer networks as the input of FADMAN and getting the results in Table 2. In this case, FADMAN (BJ)-6 denotes the experimental results for six networks from G1-G6, and FADMAN (BJ)-3 denotes the results for three networks from G4-G6. Except for the FADMAN method, the other comparison methods are non-federated anomaly detection algorithms. From Table 2, we can draw the following conclusions:

Firstly, FADMAN has reached 0.97 for Precision and 0.99 for Accuracy, which are basically the same as the non-federated methods, while protecting privacy. F1 and Recall both exceed the NPHGS method at a noise level of 30, and FNR is higher than the comparison method at all noise levels, thus showing that FADMAN not only protects well privacy, while being able to have efficient anomaly detection.

Secondly, we conducted comparison experiments on three datasets and six datasets, respectively, and it can be obtained from Table 2 that each experimental metrics of the six datasets is higher than the experimental results of the three datasets, which is because considering more information is more beneficial to capture useful information and thus improve the performance of anomaly detection.

2) Ability to detect anomalies on attributeless network: By setting the p-values of all nodes in G_6 to 1, it is regarded as an attributeless network. Then run FADMAN to get metrics in Table 3 (Higher Criticism (HC) statistic results are the same as BJ). For comparable TPR (prediction) and FNR (prediction), the FADMAN algorithm reached 0.98 and 0.02, which is significantly better than the baselines. Moreover, compared with the ASD-FT anomaly alignment algorithm, the total number of abnormal anchor links obtained by our algorithm is 1,012, which is 8.8 times than 115 of ASD-FT, which proves the effectiveness of FADMAN.

4.2 Case study in computer network dataset

Run FADMAN on computer network dataset, input all networks, and set $\alpha = 0.15$, $\sigma = 0.8$.

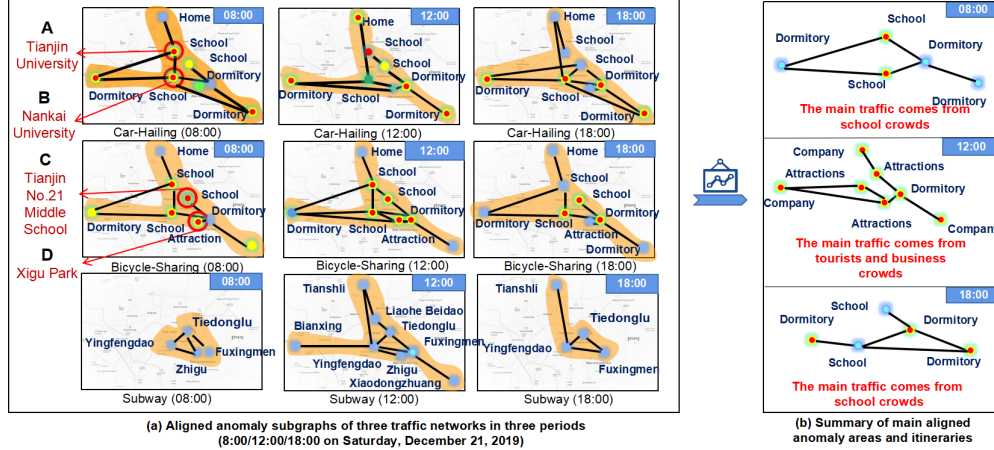


Figure 3: **Correlated abnormal distribution of Car-hailing & Bicycle-sharing & Subway detected by FadMan.** We detected the aligned anomaly subgraphs at 8:00, 12:00 and 18:00 on December 21, 2019. (a) is a heat map of the aligned abnormal distribution of the traffic networks. Each hot spot represents an abnormal area, and the redder the color, the higher the abnormality of the area. The black lines indicate that there are itineraries between the two areas, the dark blue text indicates the main position type of the start and end points of the itineraries included in the area. (c) is a summary of the aligned abnormalities at three periods in (a). From the extracted main aligned anomaly areas and itineraries, we can observe that morning and evening traffic flow mainly comes from school crowds, while at noon, it is mainly business crowds and tourists.

1) Discovery of related abnormal IP group: Our algorithm can obtain the abnormal IP group and mine the hidden attacking IP information (Figure 2). FADMAN can mine potential abnormal anchor links among multi-layer networks. By summarizing the anchor nodes corresponding to these anchor links, we can obtain an abnormal IP group. Although these IPs appear in different periods, their attack behaviors are similar. Through their log information, we found these IPs come from several fixed network segments, and their attack methods and locations are also the same, which means that these IPs may come from the same attack source. Our method finds effective cyber attacks and thus improves the prevention of cyber attacks.

2) Prediction of cyber attacks: We treat G_6 as an attributeless network by setting the p-value of all nodes in G_6 to 1 and use it with other networks as the input of FADMAN to obtain its anomaly subgraph S_6 . Regard S_6 as the prediction result, which summarizes the IPs that may attack the website during the period of G_6 . We compare it with the real attacks that occurred during this period, and get the TPR (prediction) and FNR (prediction) in Table 3. We can observe from the metrics that FADMAN can make reasonably accurate predictions of future attacks. Our algorithm can detect the abnormal situation of the target network through networks with sufficient abnormal characteristics, even if the target network does not have any abnormal information.

4.3 Case study in traffic datasets

Run FADMAN on multiple networks composed of the car-hailing itinerary network, the bicycle-sharing itinerary network, and the subway (metro) network. Match the abnormal detection results on the three traffic networks with the POI data to obtain the real information of the detection results, and then mapping it to a map. We selected three networks with the same period (8:00/12:00/18:00) and set $\alpha = 0.05$, $\sigma = 0.8$. We choose the illustrative analysis obtained on datasets of 8:00 as an example:

Discovery of real events: For the anomaly detection results of different datasets, we mapped them to the map after matching with POI data, and the obtained result graph is collectively referred to as the mapping graph below. From the mapping graph of a single dataset (Bicycle-Sharing), we can find that most of the anomalies are clustered near schools, hospitals and parks, and a small number of anomalies are also distributed around some large shopping malls. Schools, hospitals, and parks are popular places in a city in the morning. This distribution is in line with the actual situation, indicating that the obtained abnormal detection results are authentic. From the mapping graph of the two datasets (Car-Hailing & Bicycle-Sharing), The number of anomalies distributed near Xigu Park is

more than other parks. Based on this result, we searched the Weibo dataset and found that there were many posts related to Xigu Park that day, and the content of the posts were mostly records of visiting Xigu Park in the morning. Through further analysis of the detection results of the two datasets, we can find more information. Finally, from the mapping graph of the three datasets (Car-Hailing & Bicycle-Sharing & Subway), it can be found that there are many abnormal points near Tianjin University, Nankai University and Tianjin No. 21 Middle School, but there is no such situation near Tianjin No. 1 Middle School and Tianjin No. 2 Middle School. In view of this phenomenon, we consult relevant data and draw the following conclusions: In this experiment, the date of the dataset is December 21, 2019, which is the first day of the National Unified Entrance examination for Master's graduates. Therefore, the phenomenon of anomaly gathering near the school on this day is closely related to the Unified National Graduate Entrance Examination. Most of the candidates who took the exams at Tianjin University and Nankai University were students of their own schools, and their travel methods were mainly walking and riding shared bicycles. The candidates who took the exam at Tianjin No. 21 Middle School were all off-campus candidates, and their travel methods were mostly Car-Hailing, So there are a lot of anomalies around these three sites. In contrast, Tianjin No. 1 Middle School and Tianjin No. 2 Middle School are not test sites, so there are no abnormal points around them. According to the above analysis, we can find that different numbers of datasets can obtain different interpretable results. The more datasets we have, the more anomalies we can get, which is exactly what FADMAN aims to achieve.

5 Conclusion

In this paper, we study the problem of federated anomaly detection across multiple attributed networks and propose a federated learning solution, FADMAN. Our algorithm first introduces the network alignment method to the anomaly subgraph detection across multiple attributed networks, and protects private industry data. Our algorithm can be applied to detect anomalies on attributeless networks. A solid theoretical basis is developed for our algorithm.

References

- Leman Akoglu, Hanghang Tong, and Danai Koutra. Graph based anomaly detection and description: a survey. *Data mining and knowledge discovery*, 29(3):626–688, 2015.
- Mishari Almishari and Gene Tsudik. Exploring linkability of user reviews. In *European Symposium on Research in Computer Security*, pages 307–324. Springer, 2012.
- Robert H Berk and Douglas H Jones. Goodness-of-fit test statistics that dominate the kolmogorov statistics. *Zeitschrift für Wahrscheinlichkeitstheorie und verwandte Gebiete*, 47(1):47–59, 1979.
- Siddharth Bhatia, Bryan Hooi, Minji Yoon, Kijung Shin, and Christos Faloutsos. Midas: Microcluster-based detector of anomalies in edge streams. In *Proceedings of the AAAI Conference on Artificial Intelligence*, volume 34, pages 3242–3249, 2020.
- PV Bindu, P Santhi Thilagam, and Deepesh Ahuja. Discovering suspicious behavior in multilayer social networks. *Computers in Human Behavior*, 73:568–582, 2017.
- Paul Boniol and Themis Palpanas. Series2graph: Graph-based subsequence anomaly detection for time series. *Proceedings of the VLDB Endowment*, 13(12):1821–1834, 2020.
- Jose Cadena, Feng Chen, and Anil Vullikanti. Graph anomaly detection based on steiner connectivity and density. *Proceedings of the IEEE*, 106(5):829–845, 2018.
- Lei Cai, Zhengzhang Chen, Chen Luo, Jiaping Gui, Jingchao Ni, Ding Li, and Haifeng Chen. Structural temporal graph neural networks for anomaly detection in dynamic graphs. *arXiv preprint arXiv:2005.07427*, 2020.
- Feng Chen and Daniel B Neill. Non-parametric scan statistics for event detection and forecasting in heterogeneous social media graphs. In *Proceedings of the 20th ACM SIGKDD international conference on Knowledge discovery and data mining*, pages 1166–1175. ACM, 2014.

- Shengnan Chen, Jianmin Qian, Haopeng Chen, and Si Liu. Anomaly subgraph mining in large-scale social networks. In *2019 IEEE Intl Conf on Parallel & Distributed Processing with Applications, Big Data & Cloud Computing, Sustainable Computing & Communications, Social Computing & Networking (ISPA/BDCloud/SocialCom/SustainCom)*, pages 883–890. IEEE, 2019a.
- Yang Chen, Junzhe Zhang, and Chai Kiat Yeo. Network anomaly detection using federated deep autoencoding gaussian mixture model. In *International Conference on Machine Learning for Networking*, pages 1–14. Springer, 2019b.
- Xiaokai Chu, Xinxin Fan, Di Yao, Zhihua Zhu, Jianhui Huang, and Jingping Bi. Cross-network embedding for multi-network alignment. In *The World Wide Web Conference*, pages 273–284, 2019.
- Manlio De Domenico, Albert Solé-Ribalta, Elisa Omodei, Sergio Gómez, and Alex Arenas. Ranking in interconnected multilayer networks reveals versatile nodes. *Nature communications*, 6:6868, 2015.
- Kate Donahue and Jon Kleinberg. Optimality and stability in federated learning: A game-theoretic approach. *Advances in Neural Information Processing Systems*, 34, 2021.
- David Donoho, Jiashun Jin, et al. Higher criticism for detecting sparse heterogeneous mixtures. *The Annals of Statistics*, 32(3):962–994, 2004.
- Dhivya Eswaran, Christos Faloutsos, Sudipto Guha, and Nina Mishra. Spotlight: Detecting anomalies in streaming graphs. In *Proceedings of the 24th ACM SIGKDD International Conference on Knowledge Discovery & Data Mining*, pages 1378–1386, 2018.
- Yasunori Futamura, Xiucui Ye, Akira Imakura, and Tetsuya Sakurai. Spectral anomaly detection in large graphs using a complex moment-based eigenvalue solver. *ASCE-ASME Journal of Risk and Uncertainty in Engineering Systems, Part A: Civil Engineering*, 6(2):04020010, 2020.
- Mark Heimann, Haoming Shen, Tara Safavi, and Danai Koutra. Regal: Representation learning-based graph alignment. In *Proceedings of the 27th ACM international conference on information and knowledge management*, pages 117–126, 2018.
- Thanh Trung Huynh, Chi Thang Duong, Thang Huynh Quyet, Quoc Viet Hung Nguyen, Abdul Sattar, et al. Network alignment by representation learning on structure and attribute. In *Pacific Rim International Conference on Artificial Intelligence*, pages 698–711. Springer, 2019.
- Fei Jie, Chunpai Wang, Feng Chen, Lei Li, and Xindong Wu. A framework for subgraph detection in interdependent networks via graph block-structured optimization. *IEEE Access*, 8:157800–157818, 2020.
- Danai Koutra, Hanghang Tong, and David Lubensky. Big-align: Fast bipartite graph alignment. In *2013 IEEE 13th International Conference on Data Mining*, pages 389–398. IEEE, 2013.
- Martin Kulldorff. A spatial scan statistic. *Communications in Statistics-Theory and methods*, 26(6): 1481–1496, 1997.
- Batiste Le Bars and Argyris Kalogeratos. A probabilistic framework to node-level anomaly detection in communication networks. In *IEEE INFOCOM 2019-IEEE Conference on Computer Communications*, pages 2188–2196. IEEE, 2019.
- Tian Li, Anit Kumar Sahu, Ameet Talwalkar, and Virginia Smith. Federated learning: Challenges, methods, and future directions. *IEEE Signal Processing Magazine*, 37(3):50–60, 2020a.
- Tian Li, Anit Kumar Sahu, Manzil Zaheer, Maziar Sanjabi, Ameet Talwalkar, and Virginia Smith. Federated optimization in heterogeneous networks. *Proceedings of Machine Learning and Systems*, 2:429–450, 2020b.
- Tian Li, Shengyuan Hu, Ahmad Beirami, and Virginia Smith. Ditto: Fair and robust federated learning through personalization. In *International Conference on Machine Learning*, pages 6357–6368. PMLR, 2021.

- Li Liu, William K Cheung, Xin Li, and Lejian Liao. Aligning users across social networks using network embedding. In *Ijcai*, pages 1774–1780, 2016.
- Siyuan Liu, Shuhui Wang, Feida Zhu, Jinbo Zhang, and Ramayya Krishnan. Hydra: Large-scale social identity linkage via heterogeneous behavior modeling. In *Proceedings of the 2014 ACM SIGMOD international conference on Management of data*, pages 51–62, 2014.
- Lingjuan Lyu, Han Yu, and Qiang Yang. Threats to federated learning: A survey. *arXiv preprint arXiv:2003.02133*, 2020.
- Luke Mathieson, Natalie Jane de Vries, and Pablo Moscato. Using network alignment to identify conserved consumer behaviour modelling constructs. In *Business and Consumer Analytics: New Ideas*, pages 513–541. Springer, 2019.
- Luca Melis, Congzheng Song, Emiliano De Cristofaro, and Vitaly Shmatikov. Exploiting unintended feature leakage in collaborative learning. In *2019 IEEE Symposium on Security and Privacy (SP)*, pages 691–706. IEEE, 2019.
- Lin Meng, Yuxiang Ren, Jiawei Zhang, Fanghua Ye, and S Yu Philip. Deep heterogeneous social network alignment. In *2019 IEEE First International Conference on Cognitive Machine Intelligence (CogMI)*, pages 43–52. IEEE, 2019.
- Huda Nassar, Nate Veldt, Shahin Mohammadi, Ananth Grama, and David F Gleich. Low rank spectral network alignment. In *Proceedings of the 2018 World Wide Web Conference*, pages 619–628, 2018.
- Chien-Chun Ni, Yu-Yao Lin, Jie Gao, and Xianfeng Gu. Network alignment by discrete ollivier-ricci flow. In *International Symposium on Graph Drawing and Network Visualization*, pages 447–462. Springer, 2018.
- Simon Parkinson, Mauro Vallati, Andrew Crampton, and Shirin Sohrabi. Graphbad: A general technique for anomaly detection in security information and event management. *Concurrency and Computation: Practice and Experience*, 30(16):e4433, 2018.
- Daniele Perito, Claude Castelluccia, Mohamed Ali Kaafar, and Pere Manils. How unique and traceable are usernames? In *International Symposium on Privacy Enhancing Technologies Symposium*, pages 1–17. Springer, 2011.
- Skyler Speakman, Yating Zhang, and Daniel B Neill. Dynamic pattern detection with temporal consistency and connectivity constraints. In *2013 IEEE 13th International Conference on Data Mining*, pages 697–706. IEEE, 2013.
- Skyler Speakman, Edward McFowland III, and Daniel B Neill. Scalable detection of anomalous patterns with connectivity constraints. *Journal of Computational and Graphical Statistics*, 24(4): 1014–1033, 2015.
- Li Sun, Zhongbao Zhang, Pengxin Ji, Jian Wen, Sen Su, and S Yu Philip. Dna: Dynamic social network alignment. In *2019 IEEE International Conference on Big Data (Big Data)*, pages 1224–1231. IEEE, 2019.
- Ying Sun, Wenjun Wang, Nannan Wu, Wei Yu, and Xue Chen. Anomaly subgraph detection with feature transfer. In *Proceedings of the 29th ACM International Conference on Information and Knowledge Management (CIKM’20), October 19–23, 2020, Virtual Event, Ireland.*, 2020.
- Maciej Szmít, Anna Szmít, Sławomir Adamus, and Sebastian Bugała. Usage of holt-winters model and multilayer perceptron in network traffic modelling and anomaly detection. *Informatica*, 36(4), 2012.
- Kunihiko Takahashi, Martin Kulldorff, Toshiro Tango, and Katherine Yih. A flexibly shaped space-time scan statistic for disease outbreak detection and monitoring. *International Journal of Health Geographics*, 7(1):14, 2008.
- Nguyen Thanh Tam, Matthias Weidlich, Bolong Zheng, Hongzhi Yin, Nguyen Quoc Viet Hung, and Bela Stantic. From anomaly detection to rumour detection using data streams of social platforms. *Proceedings of the VLDB Endowment*, 12(9):1016–1029, 2019.

- Jan Vosecky, Dan Hong, and Vincent Y Shen. User identification across multiple social networks. In *2009 first international conference on networked digital technologies*, pages 360–365. IEEE, 2009.
- Bo Wang, Yanping Zhao, Fengye Hu, and Ying-Chang Liang. Anomaly detection with subgraph search and vertex classification preprocessing in chung-lu random networks. *IEEE Transactions on Signal Processing*, 66(20):5255–5268, 2018a.
- Chenxu Wang, Zhiyuan Zhao, Yang Wang, Dong Qin, Xiapu Luo, and Tao Qin. Deepmatching: A structural seed identification framework for social network alignment. In *2018 IEEE 38th International Conference on Distributed Computing Systems (ICDCS)*, pages 600–610. IEEE, 2018b.
- Nannan Wu, Feng Chen, Jianxin Li, Jinpeng Huai, Baojian Zhou, Naren Ramakrishnan, et al. A nonparametric approach to uncovering connected anomalies by tree shaped priors. *IEEE Transactions on Knowledge and Data Engineering*, 31(10):1849–1862, 2018.
- Han Xie, Jing Ma, Li Xiong, and Carl Yang. Federated graph classification over non-iid graphs. *Advances in Neural Information Processing Systems*, 34, 2021.
- Yuchen Yan, Si Zhang, and Hanghang Tong. Bright: A bridging algorithm for network alignment. In *Proceedings of the Web Conference 2021*, pages 3907–3917, 2021.
- Qiang Yang, Yang Liu, Tianjian Chen, and Yongxin Tong. Federated machine learning: Concept and applications. *ACM Trans. Intell. Syst. Technol.*, 10(2):12:1–12:19, 2019. doi: 10.1145/3298981. URL <https://doi.org/10.1145/3298981>.
- Rui Ye, Xin Li, Yujie Fang, Hongyu Zang, and Mingzhong Wang. A vectorized relational graph convolutional network for multi-relational network alignment. In *IJCAI*, pages 4135–4141, 2019.
- ZHAO Ying, WANG LiBao, CHEN JunJun, and TENG Jian. Network anomaly detection based on federated learning. *Journal of Beijing University of Chemical Technology*, 48(2):92, 2021.
- Jiawei Zhang and S Yu Philip. Multiple anonymized social networks alignment. In *2015 IEEE International Conference on Data Mining*, pages 599–608. IEEE, 2015.
- Jie Zhang, Nannan Wu, Wenjun Wang, Ying Sun, and Siddharth Bhatia. Anomaly alignment across multiple attributed networks. 2018.
- Ke Zhang, Carl Yang, Xiaoxiao Li, Lichao Sun, and Siu Ming Yiu. Subgraph federated learning with missing neighbor generation. *Advances in Neural Information Processing Systems*, 34, 2021.
- Yutao Zhang, Jie Tang, Zhilin Yang, Jian Pei, and Philip S Yu. Cosnet: Connecting heterogeneous social networks with local and global consistency. In *Proceedings of the 21th ACM SIGKDD International Conference on Knowledge Discovery and Data Mining*, pages 1485–1494, 2015.
- Ying Zhao, Junjun Chen, Di Wu, Jian Teng, and Shui Yu. Multi-task network anomaly detection using federated learning. In *Proceedings of the tenth international symposium on information and communication technology*, pages 273–279, 2019.
- Ying Zhao, Junjun Chen, Qianling Guo, Jian Teng, and Di Wu. Network anomaly detection using federated learning and transfer learning. In *International Conference on Security and Privacy in Digital Economy*, pages 219–231. Springer, 2020.
- Ligeng Zhu, Zhijian Liu, and Song Han. Deep leakage from gradients. In H. Wallach, H. Larochelle, A. Beygelzimer, F. d'Alché-Buc, E. Fox, and R. Garnett, editors, *Advances in Neural Information Processing Systems*, volume 32. Curran Associates, Inc., 2019. URL <https://proceedings.neurips.cc/paper/2019/file/60a6c4002cc7b29142def8871531281a-Paper.pdf>.

A Appendix

A.1 Related work

Our work is related to anomaly detection and network alignment. Here, we briefly introduce the related work in these two aspects.

Anomaly detection Anomaly detection has always been the focus of attention. Point anomalies only assign outliers to nodes, which can be regarded as a binary 0/1 classification problem [Akoglu et al., 2015, Wang et al., 2018a, Eswaran et al., 2018], and there is no connection between the detected abnormal nodes. However, with the expansion of anomaly detection in the field of graphics and the needs of actual scenes, abnormal nodes usually need to be displayed as connected subgraphs. On the other hand, the discovery of anomalies is often inseparable from statistical data. Compared with traditional parameterized scanning statistics (Kulldorff statistical data [Kulldorff, 1997]), nonparametric graph scan statistics (NPGS) can be applied to heterogeneous graph data because it is free of distribution assumption. Therefore, many NPGS-based abnormal connected subgraph detection algorithms were born in combination with actual scenarios and performance requirements. They can be divided into exact algorithms [Takahashi et al., 2008, Speakman et al., 2015, Le Bars and Kalogeratos, 2019] and approximate algorithms [Chen and Neill, 2014, Wu et al., 2018, Speakman et al., 2013]. Among them, Wu.etal proved that anomaly subgraph detection is an NP-hard problem, and proposed TSPSD [Wu et al., 2018] based on dynamic programming[Cadena et al., 2018, Bhatia et al., 2020, Cai et al., 2020, Boniol and Palpanas, 2020]. The algorithm approximates the graph to a tree topology and can be used for the large-scale dataset. Most of these algorithms are used in a single network, and only a few are used in multi-layer network scenarios [Bindu et al., 2017, De Domenico et al., 2015, Tam et al., 2019, Jie et al., 2020], and they are all used to identify abnormal nodes, not subgraphs. To the best of our knowledge, the latest work used to detect multiple networks' anomaly subgraphs is ASD-FT [Sun et al., 2020]. It is a method of detecting anomaly subgraphs of the graph based on anomaly features of another graph. It introduces the basic idea of network alignment to capture anomaly features' transmission by inferring the basic edges between multiple entity networks. However, it is suitable for two network scenarios, which is different from our work.

Network alignment Network alignment is the basic problem of cross-network mining, and many papers have proposed solutions. Most of them are based on attributes and structure. Traditional methods [Perito et al., 2011, Vosecky et al., 2009, Nassar et al., 2018, Mathieson et al., 2019] mostly use entity tag information to achieve alignment, such as user nicknames in social networks and entity names in knowledge graphs. Manually defining features is another method [Almishari and Tsudik, 2012, Ni et al., 2018]. This method needs to carefully design features manually for specific problems, and it is not easy to migrate to other scenarios. Most of the above two types of methods only consider attribute information, while some methods consider both network structure and attribute information (COSNET [Zhang et al., 2015], HYDRA [Liu et al., 2014], REGAL [Heimann et al., 2018][Ye et al., 2019, Huynh et al., 2019, Yan et al., 2021]). They want to complement the network structure and attribute information to achieve a better alignment effect. Moreover, there are many network alignment studies based on deep learning[Sun et al., 2019, Wang et al., 2018b, Meng et al., 2019]. In addition, because the attribute information may be falsely fabricated or lost or hidden due to privacy, there are many alignment algorithms based only on structural information (BigAlign [Koutra et al., 2013], UMA [Zhang and Philip, 2015], IONE [Liu et al., 2016], CrossMNA [Chu et al., 2019]). Among them, UMA, REGAL, and CrossMNA can be applied to multiple network scenarios. Nevertheless, UMA and REGAL follow the assumption of topological consistency and cannot handle networks with different structures. However, CrossMNA does not follow topological consistency and can learn a common structure across network diversity. By integrating information from different networks, enhances the effect of embedding and effectively reduces space overhead, so it is suitable for large-scale multi-network scenarios.

Our work is based on the TSPSD and CrossMNA algorithms. Compared with the existing work, we are innovative and superior to the baselines in terms of efficiency and comprehensiveness.

A.2 Two non-parametric graph scan statistics

A data owner has an attributed network $G = (V, E, P)$, $V = \{v_1, \dots, v_n\}$, $E \subseteq V \times V$ are sets of vertices and edges in G , and $P \in \mathbb{R}^n$ is the specific anomaly feature set of G . P is widely obtained

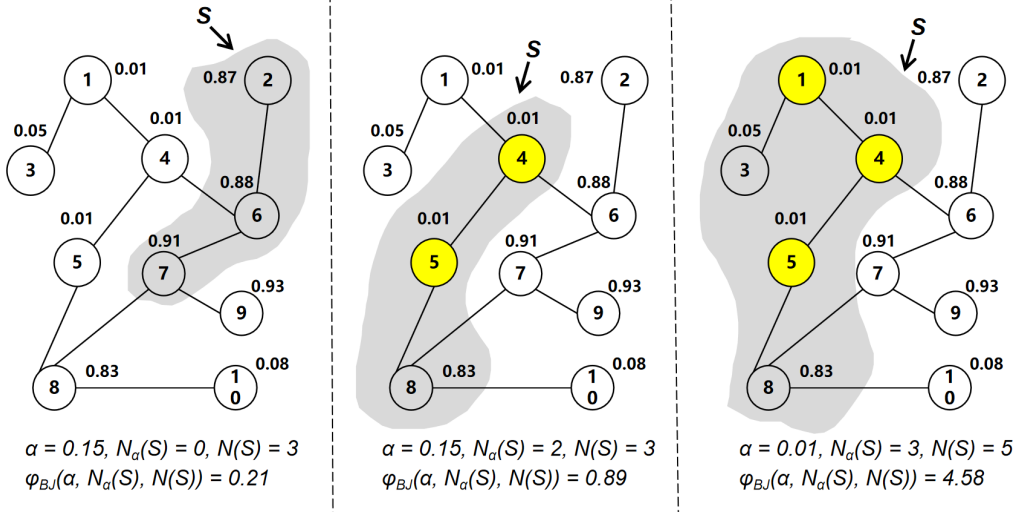


Figure 4: The BJ statistical scores for the three example subgraphs show that the score function increases with $N_\alpha(S)$ and decreases with $N(S) - N_\alpha(S)$ and α . Yellow points are the vertices with p-values less than or equal to α .

by the mapping function $\mathbf{p} : V \rightarrow [0, 1]$ defines the empirical p-value corresponding to each node $v \in V$ [Wu et al., 2018, Chen and Neill, 2014], the smaller the p-value, the more abnormal the node. Anomaly target detection can be represented as identifying subgraphs $S \subseteq G$ whose vertex set V_S and edge set E_S are subset of V, E .

Intersection of subgraphs Subgraph $S_1 \subseteq G$ whose vertex set V_{S_1} and edge set E_{S_1} are subset of V, E . Subgraph $S_2 \subseteq G$ whose vertex set V_{S_2} and edge set E_{S_2} are subset of V, E . S is the intersection set of S_1 and S_2 , where $V_S = V_{S_1} \cap V_{S_2}, E_S = E_{S_1} \cap E_{S_2}$.

Union of subgraphs Subgraph $S_1 \subseteq G$ whose vertex set V_{S_1} and edge set E_{S_1} are subset of V, E . Subgraph $S_2 \subseteq G$ whose vertex set V_{S_2} and edge set E_{S_2} are subset of V, E . S is the union set of S_1 and S_2 , where $V_S = V_{S_1} \cup V_{S_2}, E_S = E_{S_1} \cup E_{S_2}$.

Difference of subgraphs Subgraph $S_1 \subseteq G$ whose vertex set V_{S_1} and edge set E_{S_1} are subset of V, E . Subgraph $S_2 \subseteq G$ whose vertex set V_{S_2} and edge set E_{S_2} are subset of V, E . S is the difference set of S_1 and S_2 , where $V_S = V_{S_1} - V_{S_2}, E_S = E_{S_1} - E_{S_2}$.

empirical p-value The empirical p-value of node v is then defined as:

$$p(v) = \frac{1}{T} \sum_{t=1}^T I(f(v^{(t)}) \geq f(v)). \quad (8)$$

where $f(v^{(t)})$ refers to the feature vector of the node v at time t . The empirical value $p(v)$ defined above can be interpreted as the proportion of historical observations $f(v^{(t)})$ when there was no event occurring with observed values that are greater than or equal to the current observation $f(v)$.

BJ statistics Berk-Jones (BJ) statistic is defined as follows [Berk and Jones, 1979]:

$$\varphi_{BJ}(\alpha, N_\alpha(S), N(S)) = N(S) \times KL\left(\frac{N_\alpha(S)}{N(S)}, \alpha\right), \quad (9)$$

where KL is Kullback-Liebler divergence between the observed and expected proportions of p-values less than α , its formulation is presented as follows:

$$KL(a, b) = \begin{cases} a \log\left(\frac{a}{b}\right) + (1-a) \log\left(\frac{1-a}{1-b}\right), & \text{if } a \geq b \\ 0, & \text{if } a < b \end{cases} \quad (10)$$

The BJ statistic can be interpreted as the log-likelihood ratio statistic for testing whether the empirical p-value follows a uniform or piecewise constant distribution. Berk and Jones demonstrated that this statistic fulfills several optimality properties and has greater power than any weighted Kolmogorov statistic. We illustrate the BJ statistic in Figure4.

HC statistics Higher Criticism (HC) statistic is defined as follows [Donoho et al., 2004]:

$$\varphi_{HC}(\alpha, N_\alpha(S), N(S)) = \frac{N_\alpha(S) - N(S)\alpha}{\sqrt{N(S)\alpha(1-\alpha)}}. \quad (11)$$

The HC statistic can be interpreted as the log-likelihood ratio statistic for testing whether the empirical p-values follow a uniform or binomial distribution with $N(S)$ and α .

Anomalies in our experiments In the traffic datasets, anomalous nodes refer to nodes with high number of trips, the more the number of trips, the more anomalous the node is. Through experiments on traffic datasets we can conclude that the more datasets we have, the more anomaly information we get. For example, anomaly detection on one dataset can only detect the node itself as a location with high traffic such as shopping malls, hospitals, etc. On December 21, 2019, for the location hospital, anomaly detection on a single dataset can detect it as anomaly. Anomaly detection on the shared bicycle dataset only cannot detect the anomaly node of Tianjin No. 21 High School, but by performing anomaly detection on three datasets, the location can be found to be anomalous because it is a weekend and school is not in session, students living nearby usually choose shared bicycles as transportation to school instead of online cars, since this day is the first day of the National Unified Entrance examination for Master's graduates, candidates usually choose convention cars as their transportation, so this abnormal node of Tianjin No. 21 High School is detected.

A.3 Theoretical analysis

We now analyze the increasing property in the objective when one iteration of the proposed algorithm is performed. The convergence of FADMAN is proved based on several lemmas and the four properties of objective function, without the specific forms of F and Q functions. Each lemma is a building-block that describes that there exists an local optimal solution.

Theorem 6 (Convergence and Optimality of FADMAN). *Within the pre-aligned domain (each data owner integrates the alignment probability information of all node pairs between its private network and the public network), given the parameter α and σ settings, Algorithm 1 converges to the optimal solution of the problem.*

Proof. At the t -th iteration, we have the public anomaly U^t . By the step 5 at Algorithm 1, we can obtain the local optimum solution $\{S_i^t\}$.

$$\sum_{i \in [N]} F_\alpha^i(S_i^t) + Q_\sigma^i(S_i^t, U^t)$$

By the step 6 at Algorithm 1, we can obtain the new local optimum public anomaly $\{U_i^*\}$. We must upload U_i^* to the server if $Q_\sigma^i(S_i^t, U_i^*) > Q_\sigma^i(S_i^t, U^t)$, otherwise upload U^t to the server for the i -th owner. By the step 9 at Algorithm 1 and the lemma 10, we can obtain an optimum public anomaly U^* for the set $\{S_i^t\}$. Thus we have $\sum_{i \in [N]} Q_\sigma^i(S_i^t, U^*) > \sum_{i \in [N]} Q_\sigma^i(S_i^t, U^t)$. We consider U^* as the new public anomaly U^{t+1} , and we must have the following inequality:

$$\sum_{i \in [N]} F_\alpha^i(S_i^t) + Q_\sigma^i(S_i^t, U^{t+1}) > \sum_{i \in [N]} F_\alpha^i(S_i^t) + Q_\sigma^i(S_i^t, U^t)$$

As S_i^{t+1} is the local maximum solution at the step 5 at Algorithm 1, we can obtain the new inequality $\sum_{i \in [N]} F_\alpha^i(S_i^{t+1}) + Q_\sigma^i(S_i^{t+1}, U^{t+1}) > \sum_{i \in [N]} F_\alpha^i(S_i^t) + Q_\sigma^i(S_i^t, U^t)$. Algorithm 1 is repeated until the public anomaly is not changed. We obtain the optimum solution. We proved the theorem. \square

Though Theorem 6 looks straightforward to a network-based algorithm framework for federated anomaly detection, the problems at steps (c1) and (c2) can be addressed with the previous methods Sun et al. [2020], Wu et al. [2018] support the optimal solutions. At the step (c1), given the public anomaly U , the optimal private anomaly S_i^* is obtained. We are target for the new improved public anomaly U at the next iteration.

At the t -th iteration, for the server side, we can observe the public anomalies $\{U_i^*\}$ and the function values of F and Q . We assume that there exists a public anomaly subgraph $\underline{U}^* \subseteq G_0$ maximizing $\sum_{i \in [N]} Q_\sigma^i(S_i^*, U^*)$ under the fixed S_i^* . The value of $F_\alpha^i(S_i^*)$ will not change with the update U .

Lemma 7 (Q upper bound). *We must have the upper bound of the optimal Q under the fixed S_i^* .*

$$\sum_{i=1}^N Q_{\sigma}^i(S_i^*, U_i^*) \geq \sum_{i=1}^N Q_{\sigma}^i(S_i^*, U^*). \quad (12)$$

Proof. At the step 6 in Algorithm 1, we can observe that U_i^* maximizes the $Q_{\sigma}^i(S_i^*, U_i^*)$ with the fixed S_i^* . Thus for the i -th data owner, given a public anomaly U^* , we must have

$$Q_{\sigma}^i(S_i^*, U_i^*) \geq Q_{\sigma}^i(S_i^*, U^*)$$

For all of the local data owners, the inequality $\sum_{i=1}^N Q_{\sigma}^i(S_i^*, U_i^*) \geq \sum_{i=1}^N Q_{\sigma}^i(S_i^*, U^*)$ must satisfied. We proved this lemma for Q upper bound. \square

Lemma 8 (Q lower bound). *A public anomaly $U^o \subseteq \bigcup_{i \in [N]} U_i^*$ maximizes $\sum_{i \in [N]} Q_{\sigma}^i(S_i^*, U^o)$. We must have the lower bound of the optimal Q under the fixed S_i^* .*

$$\sum_{i=1}^N Q_{\sigma}^i(S_i^*, U^o) \geq \sum_{i=1}^N Q_{\sigma}^i(S_i^*, U^*). \quad (13)$$

Proof. Under the fixed S_i^* , we have already assumed that the public anomaly subgraph $U^* \subseteq G_0$ maximizing $\sum_{i \in [N]} Q_{\sigma}^i(S_i^*, U^*)$. Thus for a public anomaly subgraph $U^o \subseteq \bigcup_{i \in [N]} U_i^*$, we must have the inequality (13). This proof is proved with the intuition ways. \square

Lemma 9 (Q optimum solution). *The solution $U^o = U^*$ maximizes Q under the fixed S_i^* over G_0 . The optimum solution must exist between*

$$\min_{U \subseteq \bigcup_{i \in [N]} U_i^*} \sum_{i=1}^N \left[Q_{\sigma}^i(S_i^*, U_i^*) - Q_{\sigma}^i(S_i^*, U) \right] \quad (14)$$

Proof. Proofs of the lemma consist of two phases. At the first phase, we prove that there exists a public anomaly $U \subseteq G_0$ which minimize the gap between the Q upper bound and lower bound. According to Lemma 7 and 8, we can observe that the optimum public anomaly U must minimize the following problem:

$$\min_{U \subseteq G_0} \sum_{i=1}^N \left[Q_{\sigma}^i(S_i^*, U_i^*) - Q_{\sigma}^i(S_i^*, U) \right]$$

Next, for the phase two, we are target to prove $U = U^o = U^*$. We first assume $U = U^o \cup U^-$, where $U^o \subseteq \bigcup_{i \in [N]} U_i^*$ and $U^- \subseteq G_0 - \bigcup_{i \in [N]} U_i^*$. Then, we have the optimum solution as follows:

$$\sum_{i=1}^N \left[Q_{\sigma}^i(S_i^*, U_i^*) - Q_{\sigma}^i(S_i^*, U^o \cup U^-) \right]$$

which is equal to maximize $\sum_{i \in [N]} Q_{\sigma}^i(S_i^*, U^o \cup U^-)$. By the properties (P3) and (P4), we aim to prove that the vertices of U^- must be aligned on subset of $\{S_i^*\}$. We first assume there exist a vertex $v \in V_{U^-}$, however, the vertex v is not aligned with any vertices of $\{S_i^*\}$. Then, we must have the inequality $\sum_{i \in [N]} Q_{\sigma}^i(S_i^*, U^o \cup U^- - \{v\}) > \sum_{i \in [N]} Q_{\sigma}^i(S_i^*, U^o \cup U^-)$ by the property (P4), and the result contradicts with the maximum solution $U^o \cup U^-$. Thus all the vertices of U^- must be aligned on subset of $\{S_i^*\}$.

We assume that the public anomaly U^- is not empty. Without loss of generality, we assume there exist a vertex $v \in V_{U^-}$ which is aligned on the i -th local data owner S_i^* . We know that $v \notin V_{U_i^*}$. We must have the inequality $Q_{\sigma}^i(S_i^*, U_i^* \cup \{v\}) > Q_{\sigma}^i(S_i^*, U_i^*)$ by the property (P3), and the result contradicts with the maximum solution U_i^* . Thus the public anomaly U^- is empty. We have $U = U^o$, and prove the lemma that U^o is the optimum solution. \square

Lemma 10 (Theorem 1, from Donahue and Kleinberg [2021]). *An optimal partition Π can be created for a set of local data owners $[N]$. First, start with every owner maximizing the local public anomaly U_i^* . Then, group the owners together in ascending order of node size, halting at the first owner would increase its error $(\sum_{k \in C} |V_{U_k^*}| - |V_{U_i^*}|) / (|V_{U_i^*}| \sum_{k \in C} |V_{U_k^*}|) Q_\sigma^i(S_i^*, U_i^*)$ by joining the coalition C . The resulting partition Π is optimal.*

Proof. The public anomaly U_i^* is the local maximum solution. The Q upper bound is derived intuitively from summing local maximum solutions is greater than the global maximum solution. For the Q lower bound, the maximum solution over the local set is less than or equal the maximum solution over the global set. We can observe that the maximum solution must exist between the upper bound and lower bound, and minimize the gap between the two bounds. Note that when the gap is 0, the optimum solution is equal to the solution of lower bound. All of local solutions U_i^* are the same.

However, in the problem (14), $Q_\sigma^i(S_i^*, U)$ can not be computed at the server because the forms of function Q and private anomalies $\{S_i^*\}$ are not accessed for the data protection rules. We employ the framework for optimality and stability in federated learning to address the problem (14) Donahue and Kleinberg [2021]. We define a coalition $C \subseteq [N]$ is a subset of local data owners, and all owners $[N]$ are partitioned into coalition set $\{C\}$. We consider the gap between two bounds (14) as errors across owners. By the properties P3 and P4, we know that the value of $Q_\sigma^i(S_i^*, U)$ changed with the size of U for the fixed S_i^* . Given a partition Π of $[N]$, we define its error below:

$$f_{\{U_i^*\}}(\Pi) = \sum_{C \in \Pi} \sum_{i \in C} |V_{U_i^*}| \cdot \left(\frac{\sum_{k \in C} |V_{U_k^*}| - |V_{U_i^*}|}{|V_{U_i^*}| \cdot \sum_{k \in C} |V_{U_k^*}|} \right) Q_\sigma^i(S_i^*, U_i^*) \quad (15)$$

□

By Lemma 10, we select a coalition $C \in \Pi$ with the minimum error, and achieve the desired public anomaly $U = \bigcup_{i \in C} U_i^*$. The public anomaly U is the optimal solution for $\sum_{i \in [N]} Q_\sigma^i(S_i^*, \cdot)$.

By the theorem, our algorithm guarantees on detecting the most anomaly subgraphs on multiple private attributed networks. FADMAN's time complexity is $O(kN|V|^2)$, where k is the number of iterations, N is the number of networks, V is the number of nodes of the network. In practice, the implementations of F_α and Q_σ are normalized because the function value ranges are different.

A.4 Datasets

We constructed two multi-network scenarios based on the following five real datasets: Computer network, Car-hailing & Bicycle-sharing & Subway (Metro) & POI (Point of Interest). POI is the ground truth dataset.

(1) **Computer network:** An Internet company provided browsing logs from the **edu.cn* websites, which involved a total of 996 websites, 131,205 IPs, and the time range was from May 31, 2014 to May 31, 2015, with a total of 3,978,073 logs. In this time range, for a certain website/IP on the t -th day, we take the number of logs related to that website/IP on the t -th day as the observed value c_t . By comparing c_t with the daily c_i , ($i < t$) of the website/IP before the t -th day, the empirical p-value of the website/IP on the t -th day is obtained. Therefore, for all websites/IPs involved in the daily log, we have their corresponding p-value snapshots. We divided these logs into six parts, each containing two months of data, and constructed six computer networks based on this. (2) **Car-hailing:** We use the online car-hailing dataset provided by a transportation company. This dataset was collected 58,674 online car-hailing orders in Tianjin on December 20, 2019. Each record contains the time of the order and the start and end of the itinerary. We processed the dataset as follows: First, we divide the dataset into 24 parts according to the time (hours). For hourly data, we used the start point and endpoint of the itinerary as a node in the network and regarded the start point and endpoint of an itinerary is connected so that we can obtain the corresponding itinerary network of this hour. For the node v in the itinerary network of the hour t , we regard the number of times the node v is used as the start point or the endpoint in the hour t as the observed value c_t , and regard observed values c_i , ($i \neq t$) of v in other hours as compared values, the empirical p-value of v at hour t can be obtained. As a result, we obtained 24 car-hailing itinerary networks. (3) **Bicycle-sharing:** The dataset is also provided by a transportation company. It collected 229,814 bicycle-sharing orders in Tianjin on December 20, 2019. Each order contains time, start location, and end location. We perform the same processing

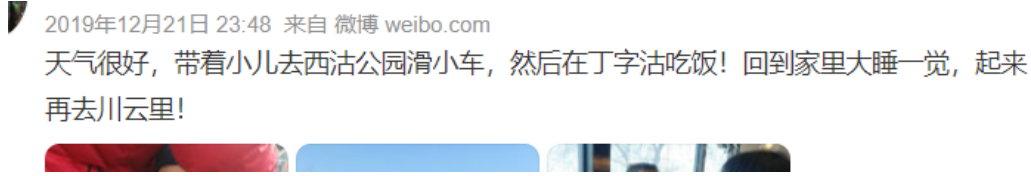


Figure 5: The translation of the weibo: Beautiful weather, took my son to Xigu Park for a little scoot, then dinner at Dingzigu! Came home for a big nap, got up and went to Chuangyunli again!



Figure 6: The translation of the weibo: I spent half an hour playing in the Xigu Park opposite my dormitory.

on this dataset as the car-hailing dataset. (4) **Subway:** This dataset collected subway traffic data in Tianjin on December 20, 2019. The data recorded the hourly passenger flow of 143 subway stations in Tianjin that day, totaling 3,432. According to the Tianjin subway route, connections are established between interconnected subway stations to form a subway network with 143 nodes and 153 edges. For the subway station s at hour t , we regard the passenger flow of s in that hour as the observed value c_t . Next, perform the same processing as the car-hailing dataset. As a result, we obtained 24 subway networks. (5) **POI:** This dataset comes from Baidu Maps, recording the information of 242,189 interest points in Tianjin. Each message contains the name, location, telephone number, longitude, latitude, id, and keyword. This dataset can map the longitude and latitude information of the Car-hailing, Bicycle-sharing, and Subway datasets to specific locations, thereby obtaining more realistic results.

A.5 Metrics

Metrics for evaluating algorithms' ability to detect correlated anomalies on multiple attributed networks: The results of FADMAN are anomaly subgraphs. The anomaly subgraph contains only a few normal nodes, most of which are abnormal. For example, if an IP has a record of attacking a website, it is identified as an abnormal node. If it is in the algorithm result, it is a true negative; otherwise, it is a false positive. For a normal node that has not attacked the website, if it is in the result, it is a false negative; otherwise, it is a true positive. We compare the results with ground truth to get these metrics. **Metrics for evaluating the algorithms' ability to detect anomalies on an attributeless network:** We regard G_6 as an attributeless network by setting p-values of its nodes to 1. We obtain the correlated anomaly subgraphs of the first five networks and their public anomaly subgraph, then align the public anomaly subgraph to G_6 to obtain the anomaly subgraph of G_6 . Anchor_Count indicates the number of real abnormal anchor links between the public anomaly subgraph and G_6 detected by the algorithm we proposed.

A.6 Weibo images in the traffic datasets case study

The Weibo images mentioned in the traffic dataset case are shown in Figure 5, 6, 7, and 8.



2019年12月21日 13:36 来自 iPhone客户端

#天津爆料#公园静悄悄，空气质量特好。西沽公园



Figure 7: The translation of the weibo: #Tianjin Explosion# The park is very quiet and the air quality is exceptionally good. Xigu Park.



2019年12月21日 14:27 来自 绿洲APP

天津西沽公园 秋景正浓 



Figure 8: The translation of the weibo: Autumn is in full swing in Tianjin Xigu Park.

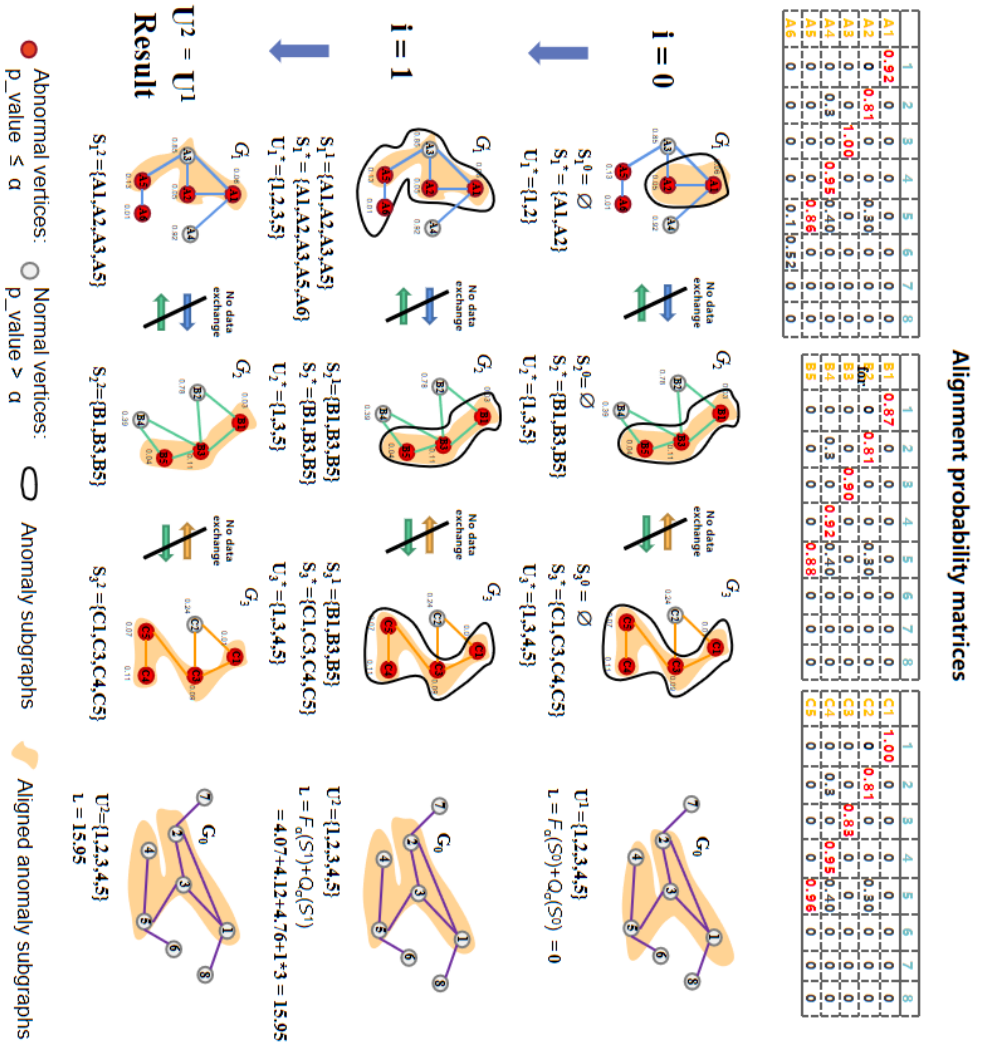
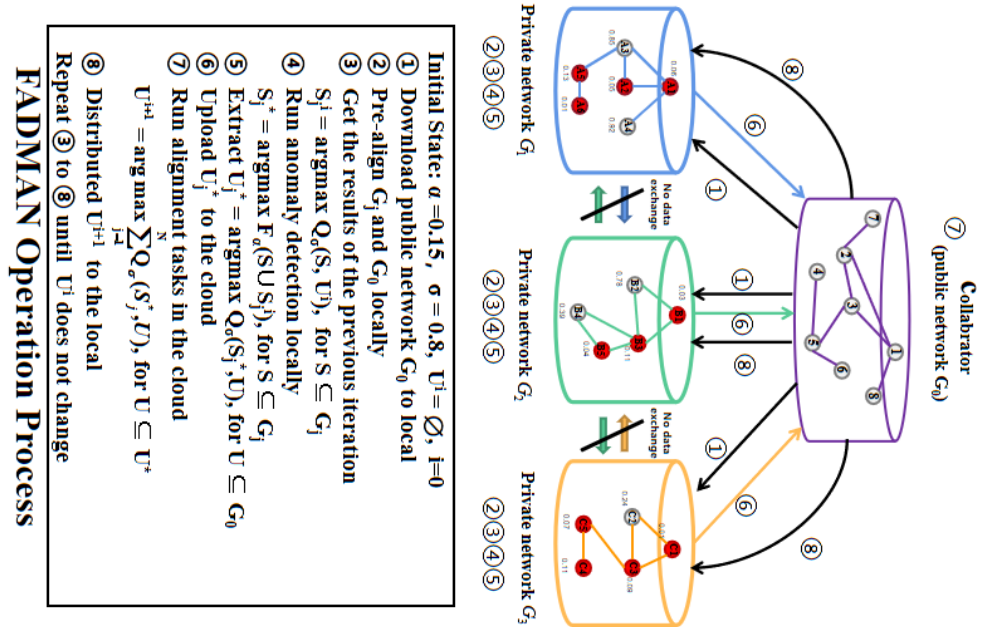


Figure 9: **Illustration of our algorithm.** The subgraphs within solid black line freeform shapes are the largest anomaly subgraphs (i.e., $\max F_\alpha$), and the yellow shaded subgraphs represent the aligned subgraphs (i.e., $\max Q_\sigma$). The vertex values are empirical p-values.